Use of an Inertia-less Virtual Synchronous Machine within Future Power Networks with High Penetrations of Converters

Mengran Yu
Andrew J. Roscoe
Campbell D. Booth
Adam Dyśko
University of Strathclyde
Glasgow, UK

Richard Ierna
Jiebei Zhu
National Grid
Warwick, UK

Helge Urdal
Urdal Power Solution Ltd
UK

***Abstract*—Conventional converter models for wind turbines and Voltage Source HVDC links, as submitted to System Operators, typically use dq-axis controllers with current injection (DQCI). Recent work carried out by the authors has proven that for DQCI converter-interfaced sources there are overall penetration limits, i.e. the 'tipping points' beyond which the system will become unstable. Initial investigations of this "tipping point", based on a reduced model of the transmission system of Great Britain using phasor simulation within DIgSILENT PowerFactory, are reviewed briefly in this paper. The 'tipping points' relating to maximum penetration of DQCI converter-interfaced sources are subsequently investigated in this paper using a higher fidelity three-phase dynamic power system model in Matlab Simulink. Additionally, a new converter controller, termed here as Virtual Synchronous Machine Zero Inertia (VSM0H), is described and implemented in the model. It is shown that, in principle, it is possible to significantly increase the penetration of converter based generation (up to 100% of installed capacity) without reaching a stability constraint.**

***Index Terms*—Virtual synchronous machine, Penetration of converters, Power system stability.**

I. INTRODUCTION

Recent work at the University of Strathclyde has shown that future alternating current (AC) power networks may become unstable unless alternative converter controller techniques are used [1]. Conventional converters for wind turbines and Voltage Source High Voltage Direct Current (HVDC) links typically use dq-axis controllers with current injection (DQCI). In these converters, active and reactive power setpoints are translated to dq-axis current (I_{dq}) references in the rotating reference frame. Inner current control loops with high bandwidth are used to control the switching bridges or multilevel modules to achieve actual injected currents closely matched to the I_{dq} references. Such converters therefore aim to have high impedances from the perspective of unbalance, harmonics, and inter-harmonics. The currents output by converter-interfaced sources aim to be close to balanced sinusoids, as required by the present GB and European Grid Codes, such as [2-4], even in the presence of voltage unbalance or harmonics. DQCI controllers are normally designed to operate in systems with a relatively low grid impedance and operate under the assumption that an infinite bus or a large positive-sequence balanced voltage source, such as a large aggregated capacity of synchronous machine (SM), is present on the network. However, in future power networks with high penetrations of renewables, such assumptions may no longer be acceptable. As the proportion of DQCI capacity rises, the effective grid impedance between the SM voltage sources and the converters increases. Eventually, a point is reached where the aggregated transient reactance (X'_d) is so large that, when it is added to the grid impedance, it causes the DQCI converters to become unstable [5, 6]. The instability is caused by the high bandwidth voltage disturbances at the point of common coupling (PCC) due to the high currents from the aggregated converters, and the large grid impedance. The frequency of the instability could typically lie anywhere within a wide frequency region, depending on the exact controller parameters, impedances, ratings/capacities, and set-points.

Reduced overall system inertia is considered to be one of the main issues that could compromise system stability under high penetration levels of converter-interfaced generation and HVDC links [7]. Swing-Equation-Based-Inertial-Response control (SEBIR) enables the converters to contribute a certain amount of additional active power during system disturbances based on the swing equation. Such supplementary control algorithms, based on the conventional DQCI converters, are widely discussed as a potential solution to system strength issues under scenarios where there are high penetrations of converters, such as [8-11]. However, the effect of SEBIR on the "tipping points" in terms of both steady-state and transient stability are unclear. The type of rate-of-change-of-frequency (RoCoF) measurement methods applied within SEBIR control schemes have a significant bearing on the performance as well as on the tipping points. Factors such as measurement time delay, dealing with harmonics, and other factors may all influence the performance and response of such schemes.

There have been various types of virtual synchronous machine (VSM) algorithms utilising converter interfaces proposed in recent years, which enable the converters to operate (to a certain degree) in a fashion similar to synchronous generators. Examples include: virtual synchronous machine (VISMA) concepts [12, 13], Synchronverter [14], virtual synchronous generator (VSG) [15, 16], power synchronisation converter [5, 17]. The current state of art of the VSM concept has been discussed in [18, 19].

As a possible alternative to SEBIR control and other established VSM algorithms, a different converter controller (based on conventional hardware design and topology) will be investigated and reported upon in this paper. This type of converter is referred to here as "VSM0H". In essence, it is a VSM algorithm that runs the switching bridge or multilevel cells (i.e. behind a filter impedance) as a balanced positive-sequence fundamental-frequency-only voltage source, with a "control" bandwidth smaller than 50 Hz so that harmonic voltages are minimized. Such converter algorithms have already been applied within marine power systems [20]. Since VSM0H converters sink or source unbalanced, harmonic or inter-harmonic currents as required, they can mitigate any point-of-common-coupling (PCC) voltage power quality deviations. It is also anticipated that system stability can be significantly improved by implementing this type of converter. This paper aims to provide a preliminary assessment of the effectiveness of VSM0H controllers in large power systems.

Recent work that explores the "tipping points", using a transmission model of the UK based on DQCI convertors using DIgSILENT PowerFactory with a positive-sequence phasor-based analysis at the 0.5 ms timestep, will be briefly summarized in section II. The "tipping points" for the penetrations of converters, using that previous analysis, will be reviewed. The principles of SEBIR control and VSM0H converter will be introduced in sections III and IV. Section V then describes a new aggregated power system model with a time step of 50 μs, implemented in Matlab SimPowerSystems. In section VI, simulation results are summarized and analysed and the effects of the following factors are on the "tipping points" and steady-state stability are explored – slope of frequency droop control of DQCI converter, implementation of SEBIR control and implementation of the VSM0H converter. Conclusions are presented in section VII.

II. REVIEW OF PREVIOUS WORK

A 37-bus equivalent network representing the National Electricity Transmission System of Great Britain (GB), have been modelled in DIgSILENT PowerFactory by National Grid (UK). The model has been dispatched in accordance with the 2030 Gone Green Scenario [21], with wind farms concentrated in Scotland and offshore, and new nuclear stations in the south of the GB power network.

A three-phase double-circuit solid fault on an interconnector between two major areas of the systems was chosen to test system stability. A sampling time step of 0.5ms is applied in the model. The results showed the tipping point for penetration of DQCI converters equates to approximately 65% in terms of transient stability and 78% in terms of steady-state stability, based on the definition of Instantaneous Penetration Level (IPL) shown in (1), where S_{NSG} is the combined MVA rating of all of the non-synchronous generation (NSG), i.e. converter-interfaced generation and HVDC links, and S_{SG} is the combined MVA rating of all synchronous generation (SG). Another common definition for IPL is the ratio of the output real power from converters to the total real power demand in the system. Corresponding tipping points based on this alternative definition are 70% and 84% respectively in terms of transient stability and steady-state stability. In this paper, the same capacity factors are assigned to each type of generation, so both definitions will result in similar values being calculated.

$$IPL\% = \frac{S_{NSG}}{S_{SG} + S_{NSG}} \times 100\% \tag{1}$$

A high-frequency (~100-300 Hz) instability phenomenon had been witnessed around the tipping points when using the PowerFactory model. The cause of this high-frequency oscillatory phenomenon is almost certainly the fast acting controllers of DQCI converters, but there is also possibility that the large sampling timestep of the simulation could have contributed to the observed instability. The exact nature of this cause will be investigated in future work. Due to the complexity and considerable simulation time required when using this model with smaller sampling timesteps, a much simplified system model has been developed in Matlab SimPowerSystems which operates with a 50 μs sampling timestep. This model will be introduced in section V.

III. SEBIR CONTROL

There have been several publications and debates addressing solutions to anticipated reductions in system strength, where various types and SEBIR implementations have been proposed to enable NSG to support system frequency recovery in response to disturbances. Work described in [8] introduces control techniques to extract stored kinetic energy from the rotating elements of wind turbine generators (WTG), and this is often termed *synthetic inertia*. Similar concepts for WTGs can also be found in other work, including [9, 10]. *Inertia emulation control* techniques for HVDC links are discussed in [11], supporting system frequency by manipulating energy stored in the DC capacitors. Other terms used in the literature include *artificial inertia*, *simulated inertia*, etc. However, the principle of all of these control techniques are invariably based on the *Swing Equation* of an SM, as shown in (2).

$$\Delta P = P_{\mathrm{m}} - P_e = \frac{2H}{f_{nom}} \frac{df}{dt} \tag{2}$$

where ΔP (in per-unit) is the amount of power imbalance in the system, P_m and P_e (in per-unit) are the mechanical and electrical power of the equivalent SM respectively, H is the per-unit inertia constant of an equivalent synchronous generator, f_{nom} is the nominal frequency of the system (in Hz) and df/dt is the RoCoF resulting from the power imbalance. When there is a power imbalance in the system, e.g. a loss of infeed event, the system frequency will drop and the RoCoF will be negative; as a result, the NSG that are equipped with SEBIR control will contribute active power to try to counteract the impact of the

original ΔP (through measuring the prevailing RoCoF) to support the system recovery. A typical configuration of a SEBIR control scheme is shown in Figure 1. A low pass filter (LPF) with a time constant τ is applied to remove high-frequency components in the ΔP signal and limit the converter ramp-rate.

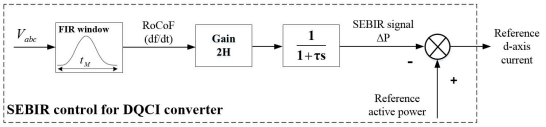

Figure 1. Configuration of SEBIR control for DQCI converter

However, it must be noted that the particular measurement methods used to measure frequency and df/dt are of great important to the performance of SEBIR control. As a fundamental component in a DQCI converter control system model, the phase locked loop (PLL) synchronises the dq axes of the converter with the network at the PCC, and allows the frequency to be measured. However, it has been shown that using a PLL to measure frequency is not always effective or accurate. Therefore, frequency measurement methods that will be investigated in this paper are those used in P and M class phase measurement units (PMU). A high level overview of such methods can be found in [22]. To measure RoCoF, the P class PMU uses a symmetric filter with a length of 3 cycles (the measuring time window length is referred as t_M in Figure 1), while the M class uses a filter with a substantially greater length of 11 cycles.

IV. VSM0H CONVERTER MODEL

The VSM0H method of controlling a converter represents a virtual synchronous machine, but with zero inertia constant *H*. Figure 2 shows a block diagram of the control philosophy, and how it relates to the 3-phase switching bridge and line filter. The main control strategy is notable in that the only measurements needed are the currents flowing from the switching bridge, I_{abc}. Additional measurements of voltages and currents at the grid-side of the filter inductor can be used for fault current limiting [23] and to optimise active and reactive power-setpoints, but these are not required for the work reported in this paper.

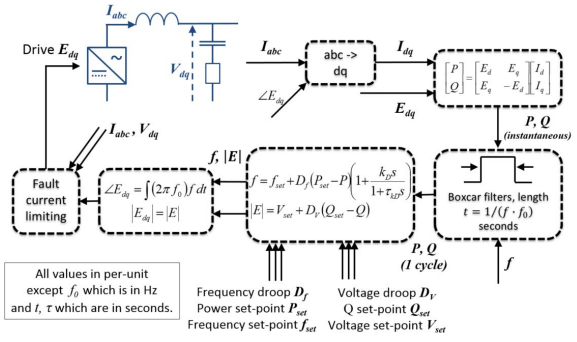

Figure 2. VSM0H converter control strategy, and single-line diagram of switching bridge and line filter

There are a number of important points to note in relation to the VSM0H controller. Firstly, it has no PLL. The phase angle of the voltage synthesised at the switching bridge is derived purely from an integrator which advances at a rate determined from a conventional droop slope of frequency versus measured active power output. Secondly, there is no inner current loop which attempts to produce sinusoidal balanced currents. Instead, the measurements of active and reactive power, averaged over 1 cycle using adaptive boxcar filters tuned to the fundamental, are used to determine target frequency and voltages using the conventional droop equations. The resulting frequency and voltages are used directly to derive the angle and magnitude of the drive voltage. Filtering the measurements of P and Q over 1 cycle is extremely useful, because when unbalance or harmonic voltages or current occur on the network, P and Q tend to ripple at twice fundamental (for unbalance) or higher frequencies for unbalanced or negative-sequence harmonics. The filtering removes these components entirely and leads to a steady values of f and |E| during scenarios of unbalance and harmonics. In this way, the converter behaves as a stable voltage source, connected to the grid via its filter impedance. The result is a converter which mitigates power quality in a very similar manner to a SG which behaves as "a voltage source behind a transient reactance" [24]. This is in contrast to the DQCI-controlled converter which has the objective of behaving as a balanced sinusoidal current source (with PLL and controller-related imperfections). This voltage-source behaviour is important, and as a consequence, the VSM0H mitigates power quality and high-frequency oscillations in the voltage waveforms at its connection point.

There is nothing in the VSM0H control strategy which attempts to introduce any synthetic inertia. In fact, if a VSM0H converter (alone) is feeding a power island and an active power load-step occurs, then the frequency would experience a rapid ramp from the initial frequency to the new frequency, as determined by the droop slope settings, over one fundamental cycle. The ramp occurs over 1 cycle due to the boxcar filtering. If the filtering was removed then the frequency ramp could in theory occur "instantly", although in practical terms this could never be measured.

Although there is no inertia, the response rapidly tracks the droop slope, with only a small time lag. As a result this control strategy does not directly mitigate against ROCOF immediately following after an event. However the frequency nadir can be well managed by the VSM0H strategy. Of course, this assumes that sufficient energy and power are available at the DC bus to provide the required response, which may be significant and is dependent on the change in the balance in load and generation.

If the boxcar filter was removed from Figure 2, and the damping term K_D set to zero, then the transfer function response of drive angle $\angle E_{dq}$ to the angle at the point-of-common coupling (PCC) $\angle V_{dq}$ evaluates as a 1st-order low-pass filter, with a time constant given by:

$$\tau = \frac{X}{2\pi f_0 D_f} \approx 8ms \tag{3}$$

By comparison the well-known response of a synchronous machine, which has inertia and damping, contains a damped 2nd-order resonance. Therefore, on first glance it certainly appears that Figure 2 provides an extremely fast-responding and stable control topology. It is not dissimilar to the "Power

Synchronisation Loop" shown in figure 8 in [5]. However, the implementation used here also includes single-cycle boxcar filtering which introduces a damped resonance into the closed-loop response (typically at ~20 Hz with $D_f = 0.04$), while being extremely beneficial for power quality. Further work is required to determine the optimal filter and parameter settings, but in this paper K_D was set to 0.002 and τ_{KD} was set to 0.001s, which slightly reduces the resonant peak. Halving the boxcar filter length to ½ cycle could completely remove the resonant peak, in conjunction with the use of K_D and τ_{KD}, but would reduce the power quality benefits for even harmonics. This will be verified in future work.

V. SIMPLIFIED POWER SYSTEM MODEL

In order to investigate the tipping points and instability phenomenon in a system model with a small time step of 50μs, a simplified power system model was built in Matlab SimPowerSystems as shown in Figure 3. This model is able to demonstrate the instability effect clearly but using only a single/aggregated SM, single/aggregated DQCI converter, network and aggregated resistive loads. Power setpoints of each type of generation can be varied to support the load in the system and the MVA rating/MW output of each type of generation can be varied to achieve different converter IPLs.

A standard SM model included in the SimPowerSystems library has been used in the model. The standard IEEEG1 steam turbine and governor model [25] and standard AC1A excitation system are applied as the control system for the synchronous generator (SG). The DQCI converter is modelled as the inverter side of a voltage source converter (VSC) based HVDC transmission system, which is connected to a DC bus with assumption of a constant and well-controlled DC link voltage. Conventional active and reactive power control of VSC-HVDC system are implemented for the DQCI converter. Additionally a frequency droop control loop is implemented to control the P setpoint and a voltage droop control loop is implemented to control the Q setpoint, both of which will be required to manage frequency and voltage if these converters are used at high penetrations. The dq-axis current references are also rate-limited to 10pu/s, which helps to manage converter start-up and HVDC link management. The VSM0H converter is based on conventional hardware design and topology but a completely different type of controller, as described in section IV. AC transmission lines are modelled as series RL circuits.

One difficult aspect of simulating high penetrations of converter-connected generation is that of initializing the simulation components, i.e. machines, governors, automatic voltage regulators (AVRs), and all converter components including PLLs and dq-axis control loops. The simulation of interest must not contain an infinite bus since frequency, voltage, and power-quality deviations from nominal are a crucial part of the simulation. In this scenario, standard techniques such as load-flow analysis for simulation initialization are not sufficient. Our approach is to start the simulation with the base load, synchronous machine(s), and an infinite bus initially connected together. Subsequently, the converter-based devices can be connected to the simulation, after their PLLs have locked and/or they are in synchronism with the rest of the network. These devices are best added in the order of most-stable first, and least-stable last. The appropriate active and reactive power set-points for each device can be estimated before the simulation, based upon the scenario load, the desired power split, and the droop slopes. However, the real simulation contains power losses, voltage drops, and line/transformer reactive power demands, which can be hard to estimate exactly until all the devices are connected and stabilised. Therefore, after all devices have been connected, small adjustments are made to the set-points, so that the active and reactive power exchange with the infinite bus reduces to almost zero. Once this is achieved, (at time = 8s in all simulations presented below), the infinite bus can be disconnected from the simulation. The simulation after that point represents the behaviour of the network in the absence of any infinite bus, which may be stable, or not.

Note that there are many factors that can affect the tipping points, in both the simulation environment and practical power systems; including system impedance, existence of harmonics, interharmonics and unbalance in the system, controller gains in DQCI converter, configuration/modelling of each type of generations, etc. In this paper, standard parameters are chosen for each component and there are no harmonics, interharmonics or unbalance considered, which will clearly affect the tipping points and system performance. These factors will be investigated in future work. It should be noted that the tipping points may vary based on these factors and different system configurations, and in this paper the tipping points demonstrated are expected to be higher than that in an actual power system or when using a more comprehensive system model.

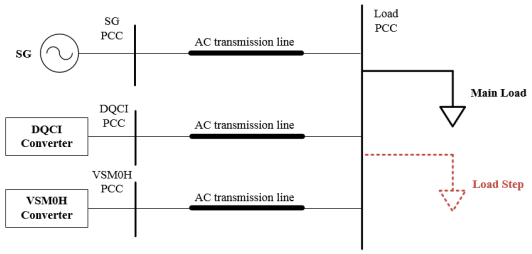

Figure 3. Configuration of simplified power system model in Matlab SimPowerSystems

VI. SIMULATION RESULTS AND DISCUSSION

Based on the simplified power system model described in section V, the tipping points of stability, in terms of DQCI converter penetration levels, are explored. Factors of interest to be investigated include the frequency droop slope of the DQCI converter, the LPF time constant in droop controllers, implementation of SEBIR control, and introduction of the VSM0H converter. To test the steady-state stability in the system, a 5% load step (with respect to the main load) is applied at 15s with a 25s total simulation time. As introduced previously, an infinite bus is applied to initialize the system and then removed at 8s after the system has initialized. At the point

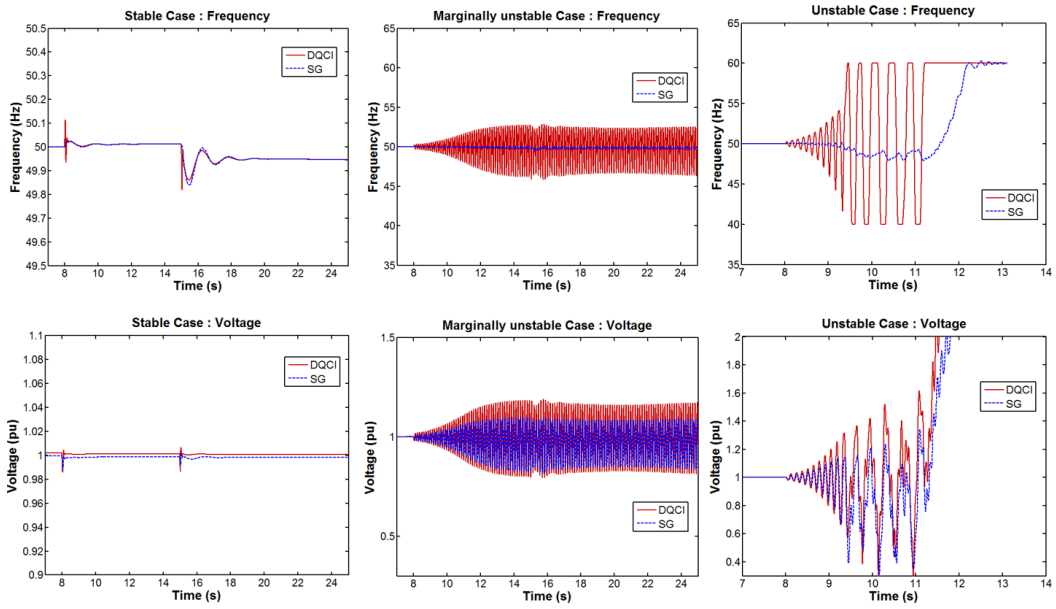

(a) Stable case (87% DQCI converter) (b) Marginally unstable (88% DQCI converter) (c) Unstable case (95% DQCI converter)

Figure 4. System performance (Frequency and voltage) under different scenarios (infinite frequency droop slope and 0.5s time constant in the LPFs applied to both frequency and voltage droop controllers in DQCI converter)

when the infinite bus is removed, there should be almost zero active and reactive power transfers to/from the infinite bus, and therefore, removing it should not introduce a significant disturbance to the system. The resistive load is set to consume 10 GW active power and 0 GVar reactive power. The rated system voltage level is 275 kV (three phase line-line voltage). The parameters of the generators and transmission lines have been populated using typical values.

In the simulations, any of the following conditions being true is interpreted as the system being either unstable or not viable:

- A locking signal from PLL in the DQCI converter is unlocked for a period of 1.5 s, any time after t=16.5 s, i.e. 1 s after the load step event;
- The frequency at the DQCI converter terminal is higher than 52 Hz or lower than 47 Hz for a period of 500 ms, based on [3, 26], at any time from t=10 s onwards (this is because in some cases, the instability occurs after the infinite bus is removed and the model cannot converge and survive until the load step event);
- The RoCoF at the DQCI converter terminal is higher than 0.5 Hz/s, at any time after t=16.5 s.

A. Case Study A : Simplified power system with only SG and DQCI converter

In this study, only SG and DQCI converters are dispatched to support system loads, where VSM0H is set to contribute 0.1% of the total load in the system and can be neglected compared to the generation of the other two types. Frequencies and terminal voltages of the generation units are measured to indicate system stability. DQCI frequency is the output frequency from the PLL in the control system and SG frequency is calculated from the machine rotor speed. The terminal voltage of the DQCI is measured from the filtered dq-axis voltage and filtered stator terminal voltage of SG is measured. With low IPL of DQCI converters in the system, i.e. below the tipping point, the system performance is expected to be stable, where the SG and DQCI converter respond satisfactorily to the load step, as shown in Figure 4(a). When IPL of DQCI converters is close to the tipping point, increasing oscillations are witnessed in the system after the load step until the RoCoF limit is reached and locking signal is found to be unlocked, where the tipping point relating to maximum DQCI converters in the system (just as instability ensues) is reached. Figure 4(b) shows a marginally unstable case, where significant oscillations are found in system frequencies, generation active power outputs and terminal voltages, which are clearly unacceptable. Under extremely high IPL of DQCI converters, it can be seen in Figure 4(c) that the system cannot even survive the initialization process with severe oscillations in an undamped manner and the model fails to converge, even before the load change is applied. It should be noted that under these conditions the frequency of the DQCI ramps between 40 Hz and 60 Hz, which is a result of the frequency limitations applied to the PLL.

The main contribution from this paper is that it is demonstrated that there are IPL limits, i.e. tipping points, in a power system with a high penetration of NSG, as shown in Table 1, and that the values of these "tipping points" are dependent on specific system characteristics. The effect of applying different frequency droop slopes to the DQCI converter has also been investigated, which can be applied to the drooped power target in a similar manner to Figure 1. The different LPF time constants τ in both frequency and voltage droop controllers are also investigated. The tipping points in terms of steady-state stability based on the simplified power system model with only SG and DQCI converter are summarized in Table 1. With different values of time constant τ in the LPFs (in both frequency and voltage droop controllers), the tipping points can vary significantly. As seen in Table 1, the tipping point can reduce from 87.8% to 51.7% with a change in

time constant from 0.5 s to 0.04 s. This suggests that allowing unfiltered dynamic droop-slope adjustments to the DQCI controller appears to have a negative effect on stability. Note that the range of time constants τ are considered according to the normal required fault clearing times at transmission levels as specified by grid codes, such as those outlined in [2]. In this paper, single-pole LPFs have been applied in the paths of droop controllers, while for converters in reality, performance of droop controllers may be affected by the combination of LPF and non-linear devices, such as ramp-rate limiter. It should be emphasised that the results shown in Table 1 are affected by both frequency and voltage droop controllers since the time constant τ is applied to both of the controllers. Effects of frequency and voltage droop controllers separately will be investigated in the future.

Table 1. Tipping points under different frequency droop slopes and time constants of droop LPFs in DQCI converter

Frequency droop slope in DQCI converter	Tipping points (%)		
	LPFs $\tau = 0.5$s	LPFs $\tau = 0.1$s	LPFs $\tau = 0.04$s
Infinite (no response to frequency)	87.8	73.0	53.8
4%	87.8	68.4	51.7

B. *Case Sudy B : Effects of SEBIR control*

By implementing different values of inertia constant and frequency measurement methods (i.e. P or M class PMU methods) in the SEBIR control, the tipping points in terms of steady-state stability have been investigated, as summarized in Table 2. Note that the SEBIR control is applied as an additional loop in the active power control system of DQCI converter. Settings of frequency droop slope in DQCI and LPF time constants are chosen to be infinite and 0.5 s respectively according to the best case in case study A. The P class PMU has a short 3-cycle measurement window for RoCoF, and so the measured value is vulnerable to disturbances and noise from transients, interharmonics, flicker and instrumentation noise. Using a P class PMU to measure either frequency or RoCoF is generally not recommended for these reasons. The M class PMU (with a reporting rate of 50 Hz) has a much longer window of 11 cycles for RoCoF, and the measured value has much lower noise and ripple due to instrumentation noise, interharmonics, and transients. With increasing inertia constant in the SEBIR control, i.e. increasing effect of SEBIR control in the system, the tipping points are expected to increase. However, Table 2 shows that the tipping points occur at lower penetrations with SEBIR engaged, than without (Table 1), either using P or M class PMUs, even though no noise, interharmonics or other poor power quality signals are simulated or introduced in this study. This result is surprising, as Table 2 suggests that the M class PMU produces slightly higher tipping points.

The reason for the reduction of achievable penetration appears to be due to the time and phase lag caused by both the RoCoF measurement process, and any other filters or ramp-rate limitations inside the DQCI converter, which includes the LPF applied in studies reported in this paper, combined with all of the other complex responses of the inner DQCI control loops and PLL responses. It appears that the SEBIR-equipped DQCI converters can act in antiphase to SG rotor oscillations, at particular "unlucky" combinations of RoCoF measurement window and filter lags, which may be difficult to predict in any real case. The results of Table 2 might look quite different if different RoCoF measurement windows or DQCI control filtering was applied. Nevertheless, it is interesting to note, that implementing SEBIR control on conventional converters may not assist system stability as expected and widely written about, but in contrast, it could possibly destabilise the system at a much lower converter penetration than would otherwise be possible.

Table 2. Tipping points with different settings in SEBIR control (infinite frequency droop slope applied in the DQCI converter)

Inertia constant (s) in SEBIR control	Tipping points (%)	
	P class PMU	M class PMU
H = 3	52.3	63.0
H = 4	47.5	59.4
H = 5	43.8	53.6

C. *Case Sudy C : Effects of VSM0H converter*

As introduced previously, The VSM0H converter employs a control algorithm which enables the converter to behave as a voltage source to the grid, while conventional DQCI converters behave as current sources in the grid. Using the simplified power system model described earlier, it has been shown that the tipping points in the system can be significantly increased, when VSM0H converter controllers are implemented in the system. LPF time constants τ are set at 0.5 s according to the best case in case study A. With VSM0H contributing 5% of the total converter-interfaced generation, the tipping point for the system without frequency droop control in the DQCI converters can be pushed up to 100%, while it can be increased by approximately 10% (to 97%) with a 4% droop. With more VSM0H, e.g. when it makes up 10% of the total generation, the model system can be stable with 100% penetration of converters, either with or without frequency droop applied to the DQCI converters. This clearly shows the potential for such a control scheme to increase penetration levels and steady state tipping points, but the effects of such control on all system characteristics must be carefully quantified before such claims can be verified.

Table 3. Tipping points with implementation of VSM0H converter

Frequency droop slope in DQCI converter	Droop LPFs τ	Tipping points (%)	
		5% VSM0H	10% VSM0H
Infinite	0.5s	100	100
4%	0.5s	96.8	100

VII. CONCLUSIONS

With increased penetration of NSG from renewable energy generation and HVDC links, power systems will be required to operate satisfactorily with higher penetrations of converters. This paper has demonstrated that the tipping points (with respect to steady-state stability) relating to the penetration of DQCI converters in a power system can be increased using

frequency droop control applied to conventional DQCI converters, but that the improvement is not significant.

SEBIR control (an often-reported promising solution to stability issues for systems with high penetrations of converters) has been implemented in the DQCI converters. By varying the inertia constant in the SEBIR control scheme and implementing different frequency measurement methods, it has been demonstrated that, while SEBIR can produce a type of inertial response, it does not help to achieve higher penetration levels. However, more detailed studies are still required to better understand the controller interactions with other control systems, series compensators and widely dispersed synchronous machines.

A new concept, the VSM0H converter controller, has been introduced and investigated using the same system model and converter architecture. It has been shown that with the use of the proposed VSM0H controller system stability can be improved significantly and that the penetration of converters can potentially reach 100% of the installed capacity without violating steady state or transient stability constraints. This initial result obtained using the simplified three-generator model in Figure 3 clearly needs further investigation. It should be noted that the tipping points do not yet include the effects of harmonics, inter-harmonics, or unbalance. Therefore, it is likely that the results are somewhat optimistic, i.e. higher than those that would be inherent in an actual power system. Additionally, the stability or instability of a particular configuration is highly dependent on the choice of many parameters (even in this simple simulation) including governors' time constants, droop slopes, network impedances and measurement time-windows. Changing just one parameter can sometimes radically alter the performance, and thus, stability limit.

Future work will investigate frequency and voltage droop controllers separately, their effects on the tipping points, system performance and tipping points in the presence of non-linear loads and under unbalanced conditions. Additionally, a wider range of combinations of droop slopes and filter parameters will be considered. Characteristics and performance of SEBIR control, VSM0H converter, and other VSM techniques will also be tested in a larger transmission model and/or the converter hardware-in-loop (CHIL) environment to more realistically establish their impact on the tipping points.

REFERENCES

[1] M. Yu, A. Dysko, C. Booth, A. Roscoe, J. Zhu, et al., "Investigations of the constraints relating to penetration of non-synchronous generation (NSG) in future power systems," in *Protection, Automation and Control (PAC) World Conference*, Glasgow, UK, 2015.

[2] National Grid (UK), "Grid Code," 2014.

[3] ENTSO-E, "Network Code for Requirements for Grid Connection Applicable to all Generators," 2015.

[4] ENTSO-E, "Network Code on High Voltage Direct Current Connections and DC-connected Power Park Modules," 2014.

[5] L. Zhang, H. Lennart, and N. H. P., "Power-Synchronization Control of Grid-Connected Voltage-Source Converters," *IEEE Transactions on Power Systems,* vol. 25, pp. 809-820, 2010.

[6] M. Durrant, H. Werner, and K. Abbott, "Model of a VSC HVDC terminal attached to a weak AC system," in *Proceedings of IEEE Conference on Control Applications*, 2003, pp. 178-182 vol.1.

[7] A. Giles, A. Roscoe, and A.-L. Olimpo, "Appropriate means of frequency measurement for the provision of inertial response from a wind turbine," in *ASRANet International Conference on Offshore Renewable Energy*, Glasgow, UK, 2014, p. 8.

[8] F. Gonzalez-Longatt, E. Chikuni, W. Stemmet, and K. Folly, "Effects of the synthetic inertia from wind power on the total system inertia after a frequency disturbance," in *Power Engineering Society Conference and Exposition in Africa (PowerAfrica), 2012 IEEE*, 2012, pp. 1-7.

[9] A. S. Overjordet, "Synthetic inertia from wind farms - Impacts on rotor angle stability in existing synchronous generators," Department of Electric Power Engineering, Norwegian University of Science and Technology, June 2014.

[10] M. Seyedi and M. Bollen, "The utilization of synthetic inertia from wind farms and its impact on existing speed governors and system performance," Report of Vindforsk Project V-369, January 2013.

[11] J. Zhu, J. M. Guerrero, W. Hung, C. D. Booth, and G. P. Adam, "Generic inertia emulation controller for multi-terminal voltage-source-converter high voltage direct current systems," *IET Renewable Power Generation,* vol. 8, pp. 740-748, 2014.

[12] H. P. Beck and R. Hesse, "Virtual synchronous machine," in *9th International Conference on Electrical Power Quality and Utilisation*, 2007, pp. 1-6.

[13] Y. Chen, R. Hesse, D. Turschner, and H.-P. Beck, "Comparison of methods for implementing virtual synchronous machine on inverters " in *International Conference on Renewable Energies and Power Quality*, Santiago de Compostela, Spain, 2012.

[14] Q.-C. Zhong and G. Weiss, "Synchronverters: Inverters That Mimic Synchronous Generators," *IEEE Transactions on Industrial Electronics,* vol. 58, pp. 1259-1267, 2011.

[15] K. Visscher and S. W. H. de Haan, "Virtual synchronous machines (VSG) for frequency stabilisation in future grids with a significant share of decentralized generation," in *IET CIRED Seminar on SmartGrids for Distribution*, 2008, pp. 1-4.

[16] K. Sakimoto, Y. Miura, and T. Ise, "Stabilization of a power system with a distributed generator by a Virtual Synchronous Generator function," in *8th IEEE International Conference on Power Electronics and ECCE Asia*, 2011, pp. 1498-1505.

[17] S. D'Arco, J. A. Suul, and O. B. Fosso, "A Virtual Synchronous Machine implementation for distributed control of power converters in SmartGrids," *Electric Power Systems Research,* vol. 122, pp. 180-197, 2015.

[18] H. Bevrani, T. Ise, and Y. Miura, "Virtual synchronous generators: A survey and new perspectives," *International Journal of Electrical Power & Energy Systems,* vol. 54, pp. 244-254, 2014.

[19] S. D'Arco and J. A. Suul, "Virtual synchronous machines - Classification of implementations and analysis of equivalence to droop controllers for microgrids," in *2013 IEEE PowerTech (POWERTECH)* Grenoble, France, 2013, pp. 1-7.

[20] "Marine and Offshore Applications of Vacon Drives," Available: http://drives.danfoss.com/industries/marine-and-offshore/, accessed 10 March 2016.

[21] National Grid (UK), "Future Energy Scenario," 2015.

[22] A. J. Roscoe, I. F. Abdulhadi, and G. M. Burt, "P and M Class Phasor Measurement Unit Algorithms Using Adaptive Cascaded Filters," *IEEE Transactions on Power Delivery,* vol. 28, pp. 1447-1459, 2013.

[23] A. J. Roscoe, G. Jackson, I. M. Elders, J. McCarthy, and G. M. Burt, "Demonstration of sustained and useful converter responses during balanced and unbalanced faults in microgrids," in *Electrical Systems for Aircraft, Railway and Ship Propulsion (ESARS), 2012*, 2012, pp. 1-6.

[24] P. C. Krause, O. Wasynczuk, S. D. Sudhoff, and S. Pekarek, "Analysis of Electric Machinery and Drive Systems," 2nd ed. Chapter 5 New York: IEEE Press, 2002, pp. 229-232.

[25] IEEE Power & Energy Society (PES), "Dynamic Models for Turbine-Governors in Power System Studies," 2013.

[26] Ofgem, "Distribution Code G59," 2015.